FLIP: a targetable mediator of resistance to radiation in non-small cell lung cancer

Kylie A. McLaughlin, Zsuzsanna Nemeth, Conor A. Bradley, Luke Humphreys, Izabela Stasik, Catherine Fenning, Joanna Majkut, Catherine Higgins, Nyree Crawford, Caitriona Holohan, Patrick G. Johnston, Timothy Harrison, Gerard G. Hanna, Karl T. Butterworth, Kevin M. Prise and Daniel B. Longley
Centre for Cancer Research and Cell Biology, Queen's University Belfast.

Acknowledgements*:* K.A. McLaughlin was supported by a studentship from the Department of Education and Learning, Northern Ireland. N. Crawford and I. Stasik were supported by the British Lung Foundation (CAN09-3 and APG11-5). C. Holohan was supported by Cancer Research UK (C212/A13721). Z. Nemeth, C. Higgins and J. Majkut were supported by the Wellcome Trust (SDDI: FLIP-FADD 099470).

Corresponding author: Dr Daniel Longley, Centre for Cancer Research and Cell Biology, Queen's University Belfast, 97 Lisburn Road, Belfast, Northern Ireland, BT9 7BL. d.longley@qub.ac.uk; Telephone: +44 2890 972762; Fax: +44 2890 972776.

Conflicts of interest: The authors declare no conflicts of interest.

Running Title: FLIP-mediated radio-resistance in NSCLC.

Keywords: Non-small cell lung cancer, FLIP, caspase-8, ionizing radiation, HDAC inhibitor.

Abstract

Resistance to radiotherapy due to insufficient cancer cell death is a significant cause of treatment failure in non-small cell lung cancer (NSCLC). The endogenous caspase-8 inhibitor, FLIP, is a critical regulator of cell death that is frequently overexpressed in NSCLC and is an established inhibitor of apoptotic cell death induced via the extrinsic death receptor pathway. Apoptosis induced by ionizing radiation (IR) has been considered to be mediated predominantly via the intrinsic apoptotic pathway; however, we found that IR-induced apoptosis was significantly attenuated in NSCLC cells when caspase-8 was depleted using RNA interference (RNAi), suggesting involvement of the extrinsic apoptosis pathway. Moreover, overexpression of wild-type FLIP, but not a mutant form that cannot bind the critical death receptor adaptor protein FADD, also attenuated IR-induced apoptosis, confirming the importance of the extrinsic apoptotic pathway as a determinant of response to IR in NSCLC. Importantly, when FLIP protein levels were down-regulated by RNAi, IR-induced cell death was significantly enhanced. The clinically relevant histone deacetylase (HDAC) inhibitors vorinostat and entinostat were subsequently found to sensitize a subset of NSCLC cell lines to IR in a manner that was dependent on their ability to suppress FLIP expression and promote activation of caspase-8. Entinostat also enhanced the anti-tumor activity of IR *in vivo*. Therefore, FLIP down-regulation induced by HDAC inhibitors is a potential clinical strategy to radio-sensitize NSCLC and thereby improve response to radiotherapy. Overall, this study provides the first evidence that pharmacological inhibition of FLIP may improve response of NCSLC to IR.

Introduction

Lung cancer is the most common cause of cancer death worldwide. Non-small cell lung cancer (NSCLC) represents approximately 80% of lung cancer deaths, with around 86,000 deaths per year in the USA (1). Radical chemo-radiotherapy is delivered with curative intent in localised and inoperable disease, but local recurrence after treatment is high, with an overall 5 year survival of 7-20% (2). The complexity of the underlying molecular mechanisms of radioresistance and tumor heterogeneity in NSCLC has hindered translation of novel therapies to clinic, and there remains an urgent need for better radiation-based treatment options in NSCLC. Recent advances in the development of molecularly-targeted therapies coupled with new technological approaches in radiotherapy delivery have created the opportunity for novel combination therapies with significant potential for improved treatment options for NSCLC (3).

Radiotherapy is currently one of the most effective cancer treatments, with over half of all cancer patients and around 76% of all lung cancer cases prescribed radiotherapy at some point in their treatment regimen (4). Although technological advances have improved pathological response rates to advanced conformal therapies compared to standard techniques, there is need to further improve therapeutic ratio by minimising the probability of complications in surrounding normal tissues (3,5). Evasion of cell death is a mechanism by which cancer cells resist anti-cancer therapy (6); targeting resistance to cell death is therefore a potential strategy to preferentially sensitize tumor cells to ionizing radiation (IR)-induced cell death and thereby improve response rates to radiotherapy in NSCLC.

One of the mechanisms by which tumors evade apoptosis is by overexpression of anti-apoptotic proteins such as the caspase-8 inhibitor FLIP, which blocks induction of apoptosis mediated by death receptors such as Fas, DR4 (TRAIL-R1) and DR5 (TRAIL-R2) (7,8). FLIP inhibits homo-dimerization, self-processing and activation of procaspase-8 at the death-inducing signalling complexes (DISCs) formed following activation of these receptors. FLIP also blocks apoptosis induced by the DISC-related cytoplasmic caspase-8-activating platforms TNFR1 Complex II and the Ripoptosome (9,10). Importantly, we have previously reported that FLIP is frequently overexpressed in NSCLC, and this overexpression correlates

with poor prognosis (11). Moreover, we and others have shown that FLIP is an important regulator of resistance to chemotherapy in a number of cancers, including NSCLC (11-14).

In this study, we investigated FLIP and caspase-8 as determinants of response to IR-induced cell death in NSCLC. We found that FLIP-mediated regulation of caspase-8-induced cell death is an important determinant of resistance to IR. Moreover, in a subset of NSCLC models, FLIP-mediated resistance to IR-induced apoptosis can be overcome by HDAC inhibitors that down-regulate FLIP expression. These results describe for the first time the importance of FLIP as a potentially targetable determinant of resistance to IR in NSCLC.

Materials & Methods

Reagents

Vorinostat (SAHA: suberoylanilide hydroxamic acid) and entinostat (MS-275) were purchased from Selleck Chemicals (Newmarket, UK) and were resuspended in the vehicle dimethyl sulfoxide (DMSO) at a stock concentration of 10mM. Aliquots of 100µL were stored at -20°C.

Cell lines and cell culture

The A549, NCI-H460 (H460), NCI-H1373 (H1373) and CCD-34Lu (34Lu) cell lines were obtained from ATCC (Teddington, UK) and HCC15 from the Leibniz Institute DSMZ (Braunschweig, Germany). ATCC authenticate their cell lines using Short Tandem Repeat (STR) profiling, which is a rapid, reproducible and standardized PCR-based method. DSMZ cell lines undergo authentication by DNA profiling and mycoplasma detection/elimination and their human cell lines are subjected to additional immunological, cytogenetic and molecular biological characterization. Frozen cell stocks of A549, H460 and 34Lu cell lines were obtained in November 2012, while H1373 and HCC15 cells were obtained in September 2015. After thawing, cells were maintained as previously described (15) and passaged no more than twice before new stocks were frozen down. All experiments were performed on low passage number cells. Stable FLIP overexpressing cell lines were generated as previously described (16). All cell lines were regularly screened for presence of mycoplasma using the

MycoAlert® Mycoplasma Detection Kit (Lonza, Basel, Switzerland).

siRNA transfections

Scrambed control (SC) siRNA, FLIP, caspase-8 and caspase-9 siRNAs were obtained from Dharmacon (Chicago, IL) and transfected as previously described (14, 17).

Western blotting and Antibodies

Cells were harvested and lysed in RIPA buffer and Western blotting was carried out as previously described (17). Antibodies used: FLIP (NF6) and caspase-8 (12F5) (both Alexis Biochemicals, San Diego, CA), Caspase 9 (Cell Signaling Technology, Beverly, MA, USA PARP (eBioscience, San Diego, CA), β-actin (Sigma-Aldrich, UK).

Flow cytometry

Cell death, cell cycle distribution and cell surface death receptor expression were determined as previously described (14,17).

Caspase activity assays

Caspase-Glo® 8 and Caspase-Glo® 3/7 assays (Promega, Southampton, UK) are luciferase-based caspase activity assays. Protein cell lysates (5μg) were incubated with 25μL of Caspase-Glo® reagent in a total volume of 50μL on a 96 well plate. The plate was then incubated in the dark at room temperature with gentle agitation for 30 minutes before being analysed (Biotek Synergy 4 plate reader).

Clonogenic Assays

H460 and A549 cells were seeded at various densities in triplicate on 6 well plates. Following adherence, cells were treated with drug and/or irradiated. Plates were then incubated for 14 days until colonies formed in control wells. Cells were fixed in ice cold 70% methanol, stained with 0.4% crystal violet stain solution, and colonies were manually counted. Surviving fractions were calculated from ≥3 independent experiments. Survival fraction (SF) data after a radiation dose (*D*) are fit by a weighted, stratified, linear regression using Origin Pro version 8 according to the linear–quadratic formula: $SF=\exp(-\alpha D-\beta D^2)$.

In vitro and in vivo irradiation procedures

In vitro experiments were performed with 225 kVp X-rays generated using a X-Rad 225 generator (Precision X-ray Inc., North Bradford, CT) with a 2 mm copper filter. All quoted doses are the absorbed dose in water 50 cm from the radiation source at a dose rate of 0.591 Gy/min. *In vivo* experiments were performed using a small animal radiotherapy research platform (SARRP, Xstrahl Life Sciences, UK). Prior to cone beam computed tomography (CBCT) imaging, mice were anesthetized by intra-peritoneal injection of xylazine/ketamine. Animals were imaged at 50 kV and 0.6 mA. Treatment planning was performed using Muriplan (Xstrahl Life Sciences, UK) to achieve uniform dose distributions across the tumor target by delivering two parallel opposed 10 x 10 mm beams and avoiding critical structures. Therapeutic radiation doses were delivered 10-15 min after CT imaging. SCID mice were injected with 2 million A549 cells/flank in the dorsal position. After tumors had established (d7), mice were treated with 10 mg/kg entinostat daily for 10 days (up to d17) and a total of 12 Gy IR was delivered using parallel-opposed beams in daily 2 Gy fractions for 3 days (from d10-d12). Experimental endpoints for individual animals were defined by tumor volume exceeding 400 mm^3 or animals losing in excess of 10% of their body weight at the start of the experiment. Animals received food and water *ad libitum*. All experimental procedures were carried out in accordance with United Kingdom Home office approved protocols for *in vivo* experimentation.

Statistics

GraphPad Prism v5 software was applied for statistical analysis. Student's *t*-test and two-way analysis of variance (ANOVA) with Bonferroni post-tests were performed with labelled significance as; * denotes $0.01<P<0.05$; ** denotes $0.001<P<0.01$; *** denotes $P<0.001$.

Results

Radiation induced cell death is dependent on the extrinsic apoptotic pathway. The response to IR of two NSCLC cell line models, H460 and A549 were initially assessed. The induction and repair of DNA double strand breaks following exposure to a 1 Gy dose of IR was assessed by quantification of IR-induced γH2AX foci. γH2AX foci were rapidly induced 30 minutes post-treatment and resolved within 24 hours (Supplementary Figure 1A). In both cell lines, a decreased proportion of cells in the G1 phase of the cell cycle with corresponding increase in S and G2/M phases was observed 4-8 hours after a 2 Gy dose of IR. However, these cell cycle perturbations were also resolved at 24 h (Supplementary Figure 1B). Of note, up to 72 h post-treatment, there was relatively little cell death induction in response to 2 Gy IR as indicated by analysis of the sub-G1 apoptotic population (Supplementary Figure 1C). Increasing the dose to 5 and 8 Gy significantly increased apoptosis in H460 cells at 72 hours; however, the increase in apoptosis in A549 cells in response to these high doses was less marked (Supplementary Figure 1C). These relative contrasting sensitivities to radiation-induced apoptosis were reflected at the cell survival level, with H460 cells being more radiosensitive than A549 cells (Supplementary Figure 1D). These relative radio-sensitivities are in agreement with the published literature (18) and correlate with their relative sensitivity to TRAIL-induced apoptosis and their expression levels of FLIP (16).

Assessment of caspase activity revealed that exposure to IR results in dose-dependent increases in both caspase-8 and caspase-3/7 activity in H460 cells (Supplementary Figure 2A). Importantly, RNAi-mediated procaspase-8 depletion was demonstrated to have a significant protective effect against IR-induced apoptosis 48 (Figure 1A) and 72 hours (Supplementary Figure 2B) post treatment, suggesting the involvement of the extrinsic apoptotic pathway. In contrast, down-regulation of procaspase-9 failed to rescue apoptosis induction in response to IR in H460 cells (Figure 1B). Overexpression of either FLIP(L) or FLIP(S) inhibited IR-induced apoptosis in H460 cells, with the overexpression of FLIP(S) having the more profound effect (Figure 1C). In contrast, a mutant form of FLIP(S), in which its critical Phe114 residue is mutated to Ala rendering it incapable of binding to FADD (19), was unable to inhibit IR-induced apoptosis (Figure 1C). These effects were reflected in clonogenic survival assays, with the wild-type FLIP(L) and FLIP(S) overexpressing models

exhibiting increased radioresistance, whereas the F114A FLIP(S) overexpressing model was as radiosensitive as the Empty Vector (EV) control cell line (Figure 1C and D). These results indicate that FLIP- and FADD-dependent caspase-8 activation regulate IR-induced apoptosis in this NSCLC cell line model.

FLIP siRNA synergizes with IR to induce apoptosis. To further assess the role of FLIP in regulating IR-induced apoptosis, we down-regulated both major splice forms using a pan-FLIP-targeting siRNA (FT). Consistent with our previous observations, simultaneous down-regulation of both FLIP splice forms induced apoptosis in H460 cells as indicated by PARP cleavage (Figure 2A). IR exposure in control siRNA (SC) transfected cells induced a modest dose-dependent increase in PARP cleavage. Most notably, IR significantly enhanced the PARP cleavage observed in FLIP-depleted cells; moreover, there was as much PARP cleavage in FT siRNA transfected cells exposed to 2 Gy as those exposed to 5 and 8 Gy (Figure 2A). These results were confirmed quantitatively using caspase activity assays: silencing FLIP enhanced caspase-8 and caspase-3/7 activity in H460 cells, and this was significantly enhanced by exposure to 2 Gy, with little further increase when the IR dose was elevated (Figure 2B). Quantitative assessment of cell death induction also indicated that FLIP silencing enhanced IR-induced apoptosis; moreover, the levels of cell death were similar when FLIP was depleted before or after IR exposure (Figure 2C). In addition, clonogenic survival of FLIP-depleted irradiated H460 cells was significantly diminished compared to control siRNA transfected cells (Figure 2D).

We extended these analyses to additional NSCLC models. Similar results to those obtained in the H460 cell line were observed in A549 cells, with FLIP silencing significantly enhancing radiation-induced apoptosis and decreasing clonogenic survival (Figures 3A-B). In light of the importance of the extrinsic apoptotic pathway in regulating IR-induced cell death in A549 and H460 cells, we assessed expression of the receptors that can mediate FLIP/caspase-8-dependent apoptosis, namely TNFR1, Fas/CD95, TRAIL-R1 and TRAIL-R2. All 4 receptors were expressed on the surface of each cell line, with IR increasing expression of each receptor, most notably Fas/CD95 (Supplementary Figure 3). These results are consistent with IR-induced activation of the extrinsic apoptotic pathway.

We subsequently analyzed NSCLC cell line models harboring a mutation in the gene encoding the inflammasome subunit NLRP3, which has previously been linked to hyper-sensitivity to RNAi-mediated FLIP depletion (20). In agreement with the literature, *NLRP3* mutated HCC15 and H1373 cell lines were found to be highly sensitive to FLIP-depletion as determined by PARP cleavage (Figure 3C). Increased sensitivity to IR-induced apoptosis was difficult to assess by PARP cleavage given the extent of apoptosis induced by FLIP silencing alone; however, quantitative assessment by Annexin V/propidium iodide staining indicated that the combined effects were at least additive in these models (Figure 3D).

HDAC inhibitors down-regulate FLIP and enhance radiation-induced apoptosis. The results described above clearly indicate that FLIP down-regulation sensitizes NSCLC cells to IR-induced apoptosis. Previous reports from our group have shown that HDAC inhibitors with anti-HDAC1-3 activity are efficient suppressors of FLIP expression operating at both transcriptional and post-transcriptional levels (11). In H460 cells treated with the pan-HDAC inhibitor SAHA, FLIP(L) and FLIP(S) were down-regulated (Figure 4A). Moreover, SAHA treatment significantly sensitized H460 cells to IR-induced apoptosis, but had no impact on IR-induced apoptosis induction in the 34Lu normal lung fibroblast cell line (Figure 4B); we have previously shown that SAHA only downregulates FLIP expression in 34Lu cells at higher concentrations ($\geq$ 10μM) (11). In addition, in H460 cells pre-treated with SAHA for 6h, IR-induced caspase-3/7 activation was significantly enhanced (Figure 4C). These effects were reflected in clonogenic survival assays, which also demonstrated the radio-sensitizing effects of SAHA in the H460 cell line model (Figure 4D). Moreover, different treatment schedules of IR and SAHA were similarly effective in reducing clonogenic survival (Supplementary Figure 4A).

SAHA is also an effective inhibitor of FLIP expression in A549 cells (11) and also sensitized these cell to IR (Figure 5A and Supplementary Figure 4B). Furthermore, SAHA down-regulated FLIP expression in HCC15 cells albeit to a lesser extent than in H460 and A549 cells, but had no effect on FLIP expression in the H1373 cell line (Figure 5B). This correlated with the relative effects of SAHA/IR combinations on apoptosis induction, with HCC15 more sensitive to the combination treatment than H1373 (Figure 5C).

Given the multiple modes of action of HDAC inhibitors (21,22), we used siRNA to deplete procaspase-8 expression (Figure 5D) and FLIP overexpressing cells (Figure 5E) to assess the relative importance of the FLIP/caspase-8 axis on cell death induced by the IR/SAHA combination. We found that cell death induction was significantly inhibited by procaspase-8 depletion (Figure 5D). SAHA was unable to down-regulate expression of the exogenous FLIP proteins expressed in H460 cells (Figure 5E), due to activation of the transgenic promoter (data not shown). This allowed us to assess the importance of FLIP down-regulation for the combined effects of SAHA and IR. Notably, wild-type FLIP(S) overexpression significantly inhibited SAHA/IR-induced apoptosis, whereas the F114A mutant that has impaired ability to bind to FADD was unable to inhibit apoptosis induced by the combination treatment. FLIP(L) overexpression also inhibited apoptosis induction in response to SAHA/IR, although to a lesser extent than FLIP(S) overexpression; this may reflect the lower level of FLIP(L) overexpression compared to FLIP(S) in the models at this time. Collectively, these results demonstrate the importance of FLIP down-regulation and caspase-8 activation in mediating the effects of the SAHA/IR combination treatment.

The benzamide entinostat (MS-275/SNDX-275) is an HDAC1/2/3-selective inhibitor that has been clinically assessed in NSCLC (23). Entinostat has a significantly longer plasma half-life than the hydroxamic acid-based HDAC inhibitors such as SAHA (23). Consistent with our previous observations (11), entinostat also effectively downregulated FLIP in H460 and A549 (Figures 6A and C), and efficiently down-regulated FLIP expression in HCC15 cells, but not H1373 (Figure 5B). Moreover, similar to SAHA, entinostat enhanced IR-induced apoptosis in both H460 and A549 cell lines (Figures 6B and D). Given its relative radioresistance, we assessed whether the sensitivity of A549 cells to IR could be enhanced *in vivo* by entinostat. A549 xenografts in SCID mice were directly irradiated with a total dose of 12 Gy delivered as 3 fractions of 4 Gy over 3 days delivered using parallel opposed beam geometry using a Small Animal Radiotherapy Research Platform (SARRP) and co-treated with 10 mg/kg entinostat. Both radiation alone and entinostat alone significantly retarded tumor growth (Figure 6E). The effects of the combination treatment were similar to the individual treatments up to d28, after which the co-treatment had a greater impact on tumor growth than the single agent

treatments, suggesting that long-term growth is more efficiently suppressed by the co-treatment (Figure 6E).

Discussion

NSCLC cancer is a significant international public health burden. The prognosis for patients with NSCLC remains very poor, with overall survival after 5 years for stages Ia/b, II, IIIa, IIIb and IV disease of 49-45, 30, 14, 5 and 1% respectively (24). There is an urgent need for better treatment options. For localised and inoperable forms of the disease, radiotherapy plays a critical role; however, local recurrence after treatment is common due to radio-resistance. There are multiple mechanisms of radio-resistance, including resistance to IR-induced cell death (25,26). Improved understanding of the molecular mechanisms underpinning radio-resistance in NSCLC is needed to enable the development of novel approaches to improve the efficacy of radiation-based treatment. In this study, we have identified the anti-apoptotic protein FLIP as an important mediator of radio-resistance.

FLIP is a key regulator of apoptosis that heterodimerizes with procaspase-8 at the death-inducing signalling complexes (DISCs) formed following ligation of death receptors such as TRAIL-R1 and -R2 and Fas/CD95, thereby inhibiting the homodimerization of procaspase-8 that is a prerequisite for caspase-8 activation (27). FLIP has also been demonstrated to regulate caspase-8 activation at TNFR1 Complex IIa, IIb and the Ripoptosome (28). These important complexes regulate cell fate downstream of TNFR1 ligation (Complexes IIa and b) and in response to chemotherapy and IAP antagonists (Ripoptosome) (9,29). Complexes IIb and the Ripoptosome contain RIPK1, which regulates programmed necrosis ("necroptosis") via RIPK3 and MLKL (30,31). The heterodimer formed between FLIP(L) and procaspase-8 at these complexes has enzymatic activity, which although unable to initiate apoptosis, suppresses necroptosis by cleaving RIPK1 (32). In addition to regulating apoptosis and necroptosis, FLIP has also been identified as an important regulator of autophagy through direct interactions with ATG3 (33).

Given its key roles in promoting cell survival, it is unsurprising that numerous clinical studies have demonstrated that FLIP is frequently overexpressed in cancer and that patients with

tumors with elevated levels of FLIP tend to have a poorer prognosis (34,35). We previously reported that FLIP is overexpressed in NSCLC and that high cytoplasmic FLIP expression correlates with poorer prognosis in a cohort of stage I-III NSCLC of mixed histology (roughly 50% adenomatous and 50% squamous) (11). Importantly, we and others have shown that FLIP not only inhibits apoptosis induced directly via death receptor activation, but also apoptosis induced by anti-cancer drugs in a number of cancers, including pre-clinical models of NSCLC (11,15,36); therefore, FLIP is a critical determinant of drug resistance. In contrast, there has been a lack of studies investigating the role of FLIP in regulating IR-induced apoptosis, possibly because early studies in Jurkat cells reported that FLIP was unable to prevent IR-induced apoptosis in this model (37). While some studies have unsurprisingly shown that FLIP regulates apoptosis in response to combined treatment with IR and TRAIL (38), we are aware of only one other study that has suggested a direct role of FLIP in regulating IR-induced cell death: Luo *et al*. previously reported that silencing of FLIP sensitizes HeLa cells to both radiotherapy and chemotherapy (39). However, to our knowledge there are no other studies that have evaluated the role of FLIP in modulating response to IR in NSCLC.

The current study provides strong evidence that FLIP-FADD-Caspase-8 complexes (40) are important regulators of radiation-induced cell death in pre-clinical models of NSCLC: FLIP depletion was found to enhance IR-induced apoptosis, while procaspase-8 depletion or FLIP overexpression abrogated IR-induced cell death. Moreover, FLIP's ability to inhibit IR-induced cell death was found to be dependent on its ability to interact with FADD. All of the experiments reported in this study were carried out in the absence of co-treatment with death ligands such as TRAIL and FasL/CD95L, and these models do not express detectable levels of death ligands ((33) *and unpublished observations*). Thus, the FLIP-FADD-Caspase-8 complexes induced by IR are not classical DISCs activated via the extrinsic pathway following death ligand binding. In the clinical setting, interactions between immune effector cells expressing TRAIL, FasL/CD95 and TNFα and tumor cells are likely to further enhance the importance of FLIP-FADD-Caspase-8 complexes in determining the outcome of radiotherapy.

HDAC inhibitors such as vorinostat and entinostat prevent the deacetylation of histone and non-histone proteins and have been shown to sensitise cancer cells to chemotherapy and IR (41-43). In this study, we demonstrate that HDAC inhibitors enhance the *in vitro* and *in vivo* efficacy of IR in NSCLC models. Our group previously demonstrated that HDAC inhibitors downregulate FLIP in colorectal cancer models at the post-translational level by disrupting its interaction with Ku70, resulting in FLIP ubiquitination and degradation via the ubiquitin-proteasome system (17). We also previously demonstrated that HDAC inhibitors effectively suppress FLIP expression at the transcriptional and post-transcriptional levels in H460 and A549 NSCLC cells (11). In this study, we report that HDAC inhibitors efficiently down-regulate FLIP in a subset of NSCLC pre-clinical models and that this promotes IR-induced, caspase-8-mediated apoptosis in these models.

In conclusion, we report that FLIP is a key determinant of radio-resistance in pre-clinical models of NSCLC; this is an important finding given the frequent over-expression of FLIP in this disease and suggests that FLIP expression is a potential predictive biomarker of response to radiotherapy in NSCLC. We have previously reported that procaspase-8 is also overexpressed in a significant number of NSCLCs rendering them sensitive to apoptosis when FLIP is downregulated (11,15). In this study, we demonstrate that FLIP expression can be down-regulated in at least a subset of NSCLCs using clinically relevant HDAC inhibitors and that this promotes IR-induced apoptosis. This suggests that HDAC inhibitor/IR combination therapy may be particularly effective in NSCLCs that overexpress FLIP and/or procaspase-8. This radio-sensitization approach could be combined with stereotactic delivery of radiotherapy to minimize toxicity. However, understanding the molecular determinants of HDAC inhibitor-induced down-regulation of FLIP in NSCLC will be needed to enable patient selection. As an alternative approach, small molecules that specifically target FLIP more directly than HDAC inhibitors may have wider application in combination with IR in NSCLC.

References

1. Siegel RL, Miller KD, Jemal A. Cancer statistics, 2015. CA A Cancer Journal for Clinicians. 2015;65:5–29.

2. Louie AV, Palma DA, Dahele M, Rodrigues GB, Senan S. Management of early-stage non-small cell lung cancer using stereotactic ablative radiotherapy: Controversies, insights, and changing horizons. Radiotherapy and Oncology. Elsevier Ireland Ltd; 2015;114:138–47.

3. Salama JK, Vokes EE. New radiotherapy and chemoradiotherapy approaches for non-small-cell lung cancer. Journal of Clinical Oncology. 2013;31:1029–38.

4. Delaney G, Barton M, Jacob S, Jalaludin B. A model for decision making for the use of radiotherapy in lung cancer. Lancet Oncology. 2003;4:120–8.

5. Shumway D, Corbin K, Salgia R, Hoffman P, Villaflor V, Malik RM, et al. Pathologic response rates following definitive dose image-guided chemoradiotherapy and resection for locally advanced non-small cell lung cancer. Lung Cancer. 2011;74:446–50.

6. Bernier J, Hall EJ, Giaccia A. Radiation oncology: a century of achievements. Nat Rev Cancer. 2004;4:737–47.

7. Micheau O, Shirley S, Dufour F. Death receptors as targets in cancer. Br J Pharmacol. 2013;169:1723–44.

8. Shirley S, Micheau O. Targeting c-FLIP in cancer. CANCER LETTERS. 2013;332:141–50.

9. Micheau O, Tschopp J. Induction of TNF receptor I-mediated apoptosis via two sequential signaling complexes. Cell. 2003;114:181–90.

10. Tenev T, Bianchi K, Darding M, Broemer M, Langlais C, Wallberg F, et al. The Ripoptosome, a Signaling Platform that Assembles in Response to Genotoxic Stress and Loss of IAPs. Elsevier Inc; 2011;:1–17.

11. Riley JS, Hutchinson R, McArt DG, Crawford N, Holohan C, Paul I, et al. Prognostic and therapeutic relevance of FLIP and procaspase-8 overexpression in non-small cell lung cancer. Cell Death and Disease. 2013;4:e951.

12. Micheau O, Solary E, Hammann A, Dimanche-Boitrel MT. Fas Ligand-independent, FADD-mediated Activation of the Fas Death Pathway by Anticancer Drugs. Journal of Biological Chemistry. 1999;274:7987–92.

13. Longley DB, Wilson TR, McEwan M, Allen WL, McDermott U, Galligan L, et al. c-FLIP inhibits chemotherapy-induced colorectal cancer cell death. Oncogene. 2005;25:838–48.

14. Wilson TR, McLaughlin KM, McEwan M, Sakai H, Rogers KMA, Redmond KM, et al. c-FLIP: a key regulator of colorectal cancer cell death. Cancer Research. 2007;67:5754–62.

15. Wilson TR, Redmond KM, McLaughlin KM, Crawford N, Gately K, O'Byrne K, et al. Procaspase 8 overexpression in non-small-cell lung cancer promotes apoptosis induced by FLIP silencing. Cell Death and Differentiation. 2009;16:1352–61.

16. Carson R, Celtikci B, Fenning C, Javadi A, Crawford N, Perez-Carbonell L, et al. HDAC Inhibition Overcomes Acute Resistance to MEK Inhibition in BRAF-Mutant Colorectal Cancer by Downregulation of c-FLIPL. Clin Cancer Res. 2015;21:3230–40.

17. Kerr E, Holohan C, McLaughlin KM, Majkut J, Dolan S, Redmond K, et al. Identification of an acetylation-dependant Ku70/FLIP complex that regulates FLIP expression and HDAC inhibitor-induced apoptosis. Cell Death and Differentiation. 2012;19:1317–27.

18. Tumati V, Kumar S, Yu L, Chen B, Choy H, Saha D. Effect of PF-02341066 and radiation on non-small cell lung cancer cells. Oncol Rep. 2013;29:1094–100.

19. Majkut J, Sgobba M, Holohan C, Crawford N, Logan AE, Kerr E, et al. Differential affinity of FLIP and procaspase 8 for FADD's DED binding surfaces regulates DISC assembly. Nat Comms. 2014;5:3350.

20. Kim H-S, Mendiratta S, Kim J, Pecot CV, Larsen JE, Zubovych I, et al. Systematic identification of molecular subtype-selective vulnerabilities in non-small-cell lung cancer. Cell. 2013;155:552–66.

21. Xu WS, Parmigiani RB, Marks PA. Histone deacetylase inhibitors: molecular mechanisms of action. Oncogene. 2007;26:5541–52.

22. Kim H-J, Bae S-C. Histone deacetylase inhibitors: molecular mechanisms of action and clinical trials as anti-cancer drugs. Am J Transl Res. 2011;3:166–79.

23. Knipstein J, Gore L. Entinostat for treatment of solid tumors and hematologic malignancies. Expert Opin Investig Drugs. 2011;20:1455–67.

24. American Cancer Society. *Cancer Facts & Figures 2016*. Atlanta: American Cancer Society. 2016;:1–72.

25. Willers H, Azzoli CG, Santivasi WL, Xia F. Basic mechanisms of therapeutic resistance to radiation and chemotherapy in lung cancer. Cancer J. 2013;19:200–7.

26. Chang L, Graham P, Hao J, Ni J, Deng J, Bucci J, et al. Cancer stem cells and signaling pathways in radioresistance. Oncotarget. 2015.

27. Scaffidi C, Schmitz I, Krammer PH, Peter ME. The role of c-FLIP in modulation of CD95-induced apoptosis. J Biol Chem. 1999;274:1541–8.

28. Wang L, Du F, Wang X. TNF-alpha induces two distinct caspase-8 activation pathways. Cell. 2008;133:693–703.

29. Finlay D, Vamos M, González-López M, Ardecky RJ, Ganji SR, Yuan H, et al. Small-molecule IAP antagonists sensitize cancer cells to TRAIL-induced apoptosis: roles of XIAP and cIAPs. Molecular Cancer Therapeutics. 2014;13:5–15.

30. Vandenabeele P, Declercq W, Van Herreweghe F, Vanden Berghe T. The role of the kinases RIP1 and RIP3 in TNF-induced necrosis. Science Signaling. 2010;3:re4–re4.

31. Zhao J, Jitkaew S, Cai Z, Choksi S, Li Q, Luo J, et al. Mixed lineage kinase domain-like is a key receptor interacting protein 3 downstream component of TNF-induced necrosis. Proc Natl Acad Sci USA. 2012;109:5322–7.

32. Oberst A, Dillon CP, Weinlich R, McCormick LL, Fitzgerald P, Pop C, et al. Catalytic activity of the caspase-8-FLIPL complex inhibits RIPK3-dependent necrosis. Nature. Nature Publishing Group; 2012;471:363–7.

33. Lee J-S, Li Q, Lee J-Y, Lee S-H, Jeong JH, Lee H-R, et al. FLIP-mediated autophagy regulation in cell death control. Nature Publishing Group. Nature Publishing Group; 2009;11:1355–62.

34. Salon C, Eymin B, Micheau O, Chaperot L, Plumas J, Brambilla C, et al. E2F1 induces apoptosis and sensitizes human lung adenocarcinoma cells to death-receptor-mediated apoptosis through specific downregulation of c-FLIP(short). Cell Death and Differentiation. 2006;13:260–72.

35. Ryu BK, Lee MG, Chi SG, Kim YW, Park JH. Increased expression of cFLIP(L) in colonic adenocarcinoma. J Pathol. 2001;194:15–9.

36. Day T, Najafi F, Wu C, Safa A. Cellular FLICE-like inhibitory protein (c-FLIP): A novel target for Taxol-induced apoptosis. Biochemical Pharmacology. 2006;71:1551–61.

37. Kataoka T, Schröter M, Hahne M, Schneider P, Irmler M, Thome M, et al. FLIP prevents apoptosis induced by death receptors but not by perforin/granzyme B, chemotherapeutic drugs, and gamma irradiation. J Immunol. 1998;161:3936–42.

38. Ramp U, Caliskan E, Mahotka C, Krieg A, Heikaus S, Gabbert HE, et al. Apoptosis induction in renal cell carcinoma by TRAIL and γ-radiation is impaired by deficient caspase-9 cleavage. Br J Cancer. 2003;88:1800–7.

39. Luo A, Wang W, Sima N, Lu Y, Zhou J, Xu G, et al. Short hairpin RNA targeting c-FLIP sensitizes human cervical adenocarcinoma Hela cells to chemotherapy and radiotherapy. CANCER LETTERS. 2008;271:323–32.

40. Day TW, Huang S, Safa AR. c-FLIP knockdown induces ligand-independent DR5-, FADD-, caspase-8-, and caspase-9-dependent apoptosis in breast cancer cells.

Biochemical Pharmacology. 2008;76:1694–704.

41. Camphausen K. Enhanced Radiation-Induced Cell Killing and Prolongation of γH2AX Foci Expression by the Histone Deacetylase Inhibitor MS-275. Cancer Research. 2004;64:316–21.

42. Seo S-K, Jin H-O, Woo S-H, Kim Y-S, An S, Lee J-H, et al. Histone deacetylase inhibitors sensitize human non-small cell lung cancer cells to ionizing radiation through acetyl p53-mediated c-myc down-regulation. J Thorac Oncol. 2011;6:1313–9.

43. Diyabalanage HVK, Granda ML, Hooker JM. Combination therapy: histone deacetylase inhibitors and platinum-based chemotherapeutics for cancer. Cancer Letters. 2013;329:1–8.

Figure Legends

Figure 1. IR-induced cell death in H460 cells is Caspase-8 and FLIP-dependent. **A** H460 cells were transfected with 20 nM scrambled control (SC) or caspase-8-targeted siRNA and irradiated at 2, 5 and 8 Gy. Western blotting confirmed procaspase-8 downregulation. DNA content of cells was analysed by flow cytometry and the sub-G1 population (DNA content <2N) was determined as a measurement of apoptosis 48 hours post-IR. **B** H460 cells were transfected with 20 nM scrambled control (SC), caspase-8- or caspase-9-targeted siRNA and irradiated at 2, 5 and 8 Gy. Western blotting confirmed procaspase-8 and procaspase-9 downregulation. Cell death was assessed by Annexin V/propidium iodide flow cytometry 48 hours post-IR. **C** H460 cells overexpressing wild-type FLIP(L), FLIP(S) or FLIP(S) F114A were treated with 2 or 5 Gy IR for 72 h. DNA content of cells was analysed by flow cytometry and the sub-G1 population was determined. EV denotes the control empty vector cell line. **D** Clonogenic survival assays performed in EV, FLIP(L), FLIP(S) and FLIP(S) F114A H460 cells treated with the indicated doses of IR and incubated for 14 days . A colony is defined as a group of >50 cells. Surviving fractions were calculated from 3 independent experiments, and curves were fitted using linear-quadratic model.

Figure 2. Downregulation of FLIP enhances IR-induced death in H460 cells. **A** H460 cells were transfected with 10 nM FLIP-targeted (FT) siRNA 24 h before IR and were harvested 48 h post-IR. Western blot analysis was used to detect FLIP and PARP protein expression levels. **B** Caspase-8 and caspase-3/7 activity was assessed in H460 cells transfected with 10 nM FT siRNA for 24 h prior to IR for 48 h. **C** H460 cells were transfected with 10 nM of SC or FT siRNA and treated with IR in two different schedules: IR 24 h after siRNA transfection (siFLIP/IR) or IR 24 h before transfection (IR/siFLIP). Cell death was assessed by Annexin V/propidium iodide flow cytometry 24 h after the final treatment. **D** Clonogenic survival assays performed in H460 cells transfected with FT or control siRNAs, treated with the indicated doses of IR and incubated for 14 days. Surviving fraction was calculated from 3 independent experiments, and curves were fitted using linear-quadratic model.

Figure 3. FLIP is a determinant of IR resistance in A549 and NLRP3 mutated HCC15 and H1373 NSCLC models. **A.** A549 cells were transfected with 10nM scrambled control (SC) or FLIP-targeted (FT) siRNA and treated with IR in two different schedules: IR 24 h after siRNA transfection (siFLIP/IR) or 24 h before silencing (IR/siFLIP). Cell death was assessed by Annexin V/propidium iodide method a further 24 h after the final treatment. Western blot analysis was used to confirm FT siRNA-mediated FLIP down-regulation. **B** Clonogenic survival assays performed in A549 cells transfected with FT or control siRNAs, treated with the indicated doses of IR and incubated for 14 days. Surviving fraction was calculated from 3 independent experiments, and curves were fitted using linear-quadratic model. **C** Western blot analysis of FLIP expression and PARP cleavage in HCC15 and H1373 *NLRP3* mutant NSCLC cell lines cells transfected with 10 nM FT siRNA for 6 h prior to treatment with IR for 48 h. **D** Annexin V/propidium iodide assessment of apoptosis in HCC15 and H1373 cell lines transfected with 10 nM FT siRNA for 6 h prior to treatment with IR for 72 h.

Figure 4. The pan-HDAC inhibitor vorinostat (SAHA) downregulates FLIP and enhances IR-induced cell death. **A** Western blot analysis of FLIP protein expression in H460 cells treated with 1 μM SAHA for 48 h. **B** H460 and 34Lu cells were treated with the indicated doses of SAHA for 24 h prior to exposure to 5 and 8 Gy IR. The DNA content of the cells was determined 72 h post-IR by flow cytometry, and the sub-G1 apoptotic population (DNA content <2N) determined. **C** Caspase-3/7 activity in H460 cells treated with 1μM SAHA for 6 h and irradiated with the indicated doses of IR for a further 48 h. **D** Clonogenic survival assays performed in H460 cells treated with SAHA and the indicated doses of IR. The surviving fraction after 14 days was calculated from 3 independent experiments.

Figure 5. Cell death induced by IR/SAHA combination therapy is FLIP and caspase-8-dependent. **A** Annexin V/propidium iodide assessment of apoptosis in A549 cells 48 h post-IR. Cells were pre-treated with SAHA for 24 h and irradiated with the indicated doses of IR. **B** Western blot analysis of FLIP protein expression in HCC15 and H1373 cell lines treated with 1 μM SAHA for 24 h. **C** Annexin V/propidium iodide assessment of apoptosis in

HCC15 and H1373 cell lines treated with 1 μM SAHA 6 h prior to treatment with IR; cells were analysed 72 h post-IR. **D** H460 cells were transfected with 20 nM scrambled control (SC) or caspase-8 targeted siRNA. After 24 h, cells were treated with 2.5 μM SAHA and incubated for additional 24 h, after which the cells were exposed to IR. The cells were then analysed 48 h post-IR. Western blotting confirmed procaspase-8 downregulation. DNA content of the cells was determined by flow cytometry, and the sub-G1 population (DNA content < 2N) was determined as a measurement of apoptosis. **E** Empty vector (EV), FLIP(L) WT (FL) , FLIP(S) WT (FS^{WT}) and FLIP(S) F114A MT (FS^{MT}) overexpressing cells were pre-treated with 1μM SAHA and then irradiated 24 h later. The sub-G1 apoptotic population was quantified 72 h post-IR by flow cytometry.

Figure 6. The HDAC1-3 selective inhibitor entinostat enhances IR-induced cell death *in vitro* and *in vivo*. **A** Western blot analysis of FLIP protein expression in H460 cells treated with 2.5 μM entinostat for 24 h. **B.** H460 cells were treated 5 Gy of IR, after 48 h cells were then treated with 5 μM entinostat. After a further 24 h, Annexin V/propidium iodide assessment of apoptosis was performed. **C** Western blot analysis of FLIP protein expression in A549 cells treated with 2.5 μM entinostat for 72 h. **D** A549 cells were treated with 2.5 or 5 μM entinostat for 24h and then exposed to IR. After a further 48h, Annexin V/propidium iodide assessment of apoptosis was performed. **E** Assessment of A549 xenograft growth in response to individual and combined treatment with entinostat and IR. Mice were treated with 10 mg/kg entinostat daily for 10 days (up to d17) and a total of 12 Gy IR was delivered using parallel-opposed beams in daily 2 Gy fractions for 3 days (from d10-d12). The treatment volumes on d7 prior to treatment and d36 at the end of the experiment are presented.

Figure 1

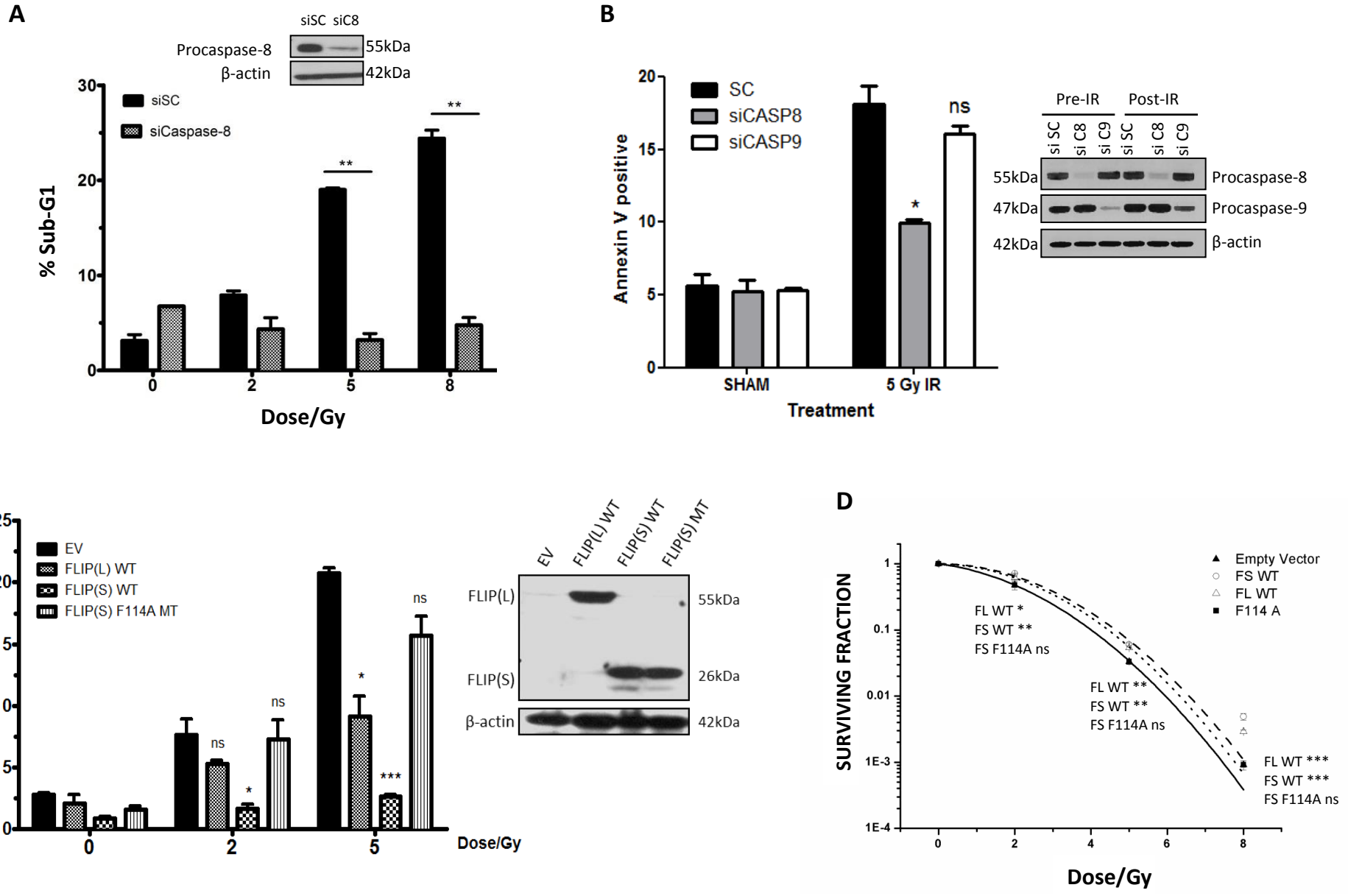
A
siSC siC8
Procaspase-8
β-actin
55kDa
42kDa
siSC
siCaspase-8
% Sub-G1
Dose/Gy
B
SC
siCASP8
siCASP9
Annexin V positive
ns
SHAM
5 Gy IR
Treatment
Pre-IR
Post-IR
si SC
si C8
si C9
55kDa
47kDa
42kDa
Procaspase-8
Procaspase-9
β-actin
C
EV
FLIP(L) WT
FLIP(S) WT
FLIP(S) F114A MT
% Sub-G1
Dose/Gy
FLIP(L)
FLIP(S)
β-actin
55kDa
26kDa
42kDa
D
SURVIVING FRACTION
Empty Vector
FS WT
FL WT
F114 A
FL WT *
FS WT **
FS F114A ns
FL WT **
FS WT **
FS F114A ns
FL WT ***
FS WT ***
FS F114A ns
Dose/Gy

Figure 2

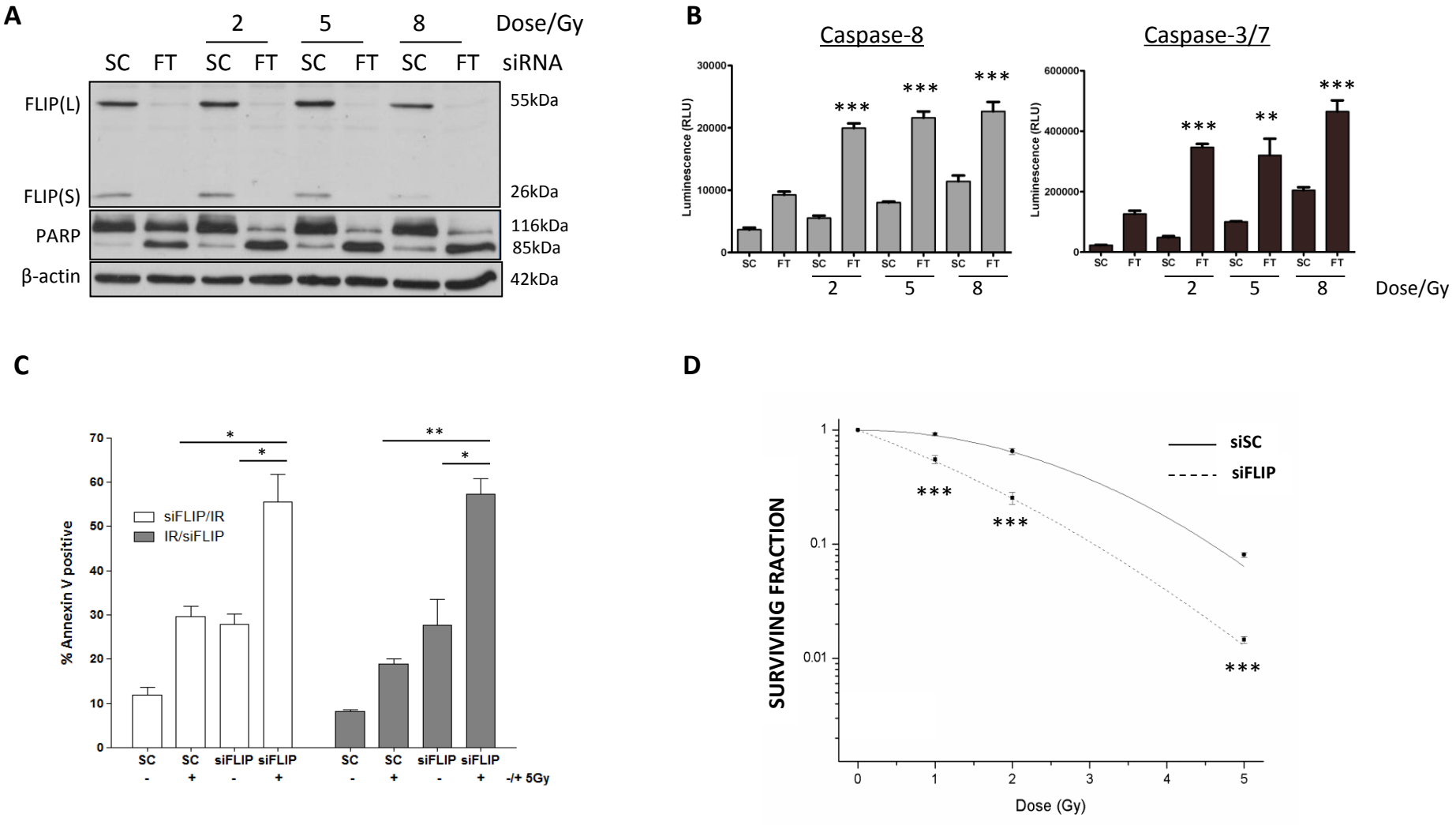
A
2
5
8
Dose/Gy
SC FT SC FT SC FT SC FT siRNA
FLIP(L)
FLIP(S)
PARP
β-actin
55kDa
26kDa
116kDa
85kDa
42kDa
B
Caspase-8
Caspase-3/7
Luminescence (RLU)
SC FT SC FT SC FT SC FT
2 5 8
Dose/Gy
C
% Annexin V positive
siFLIP/IR
IR/siFLIP
SC SC siFLIP siFLIP SC SC siFLIP siFLIP
- + - + - + - + -/+ 5Gy
D
SURVIVING FRACTION
siSC
siFLIP
Dose (Gy)

Figure 3

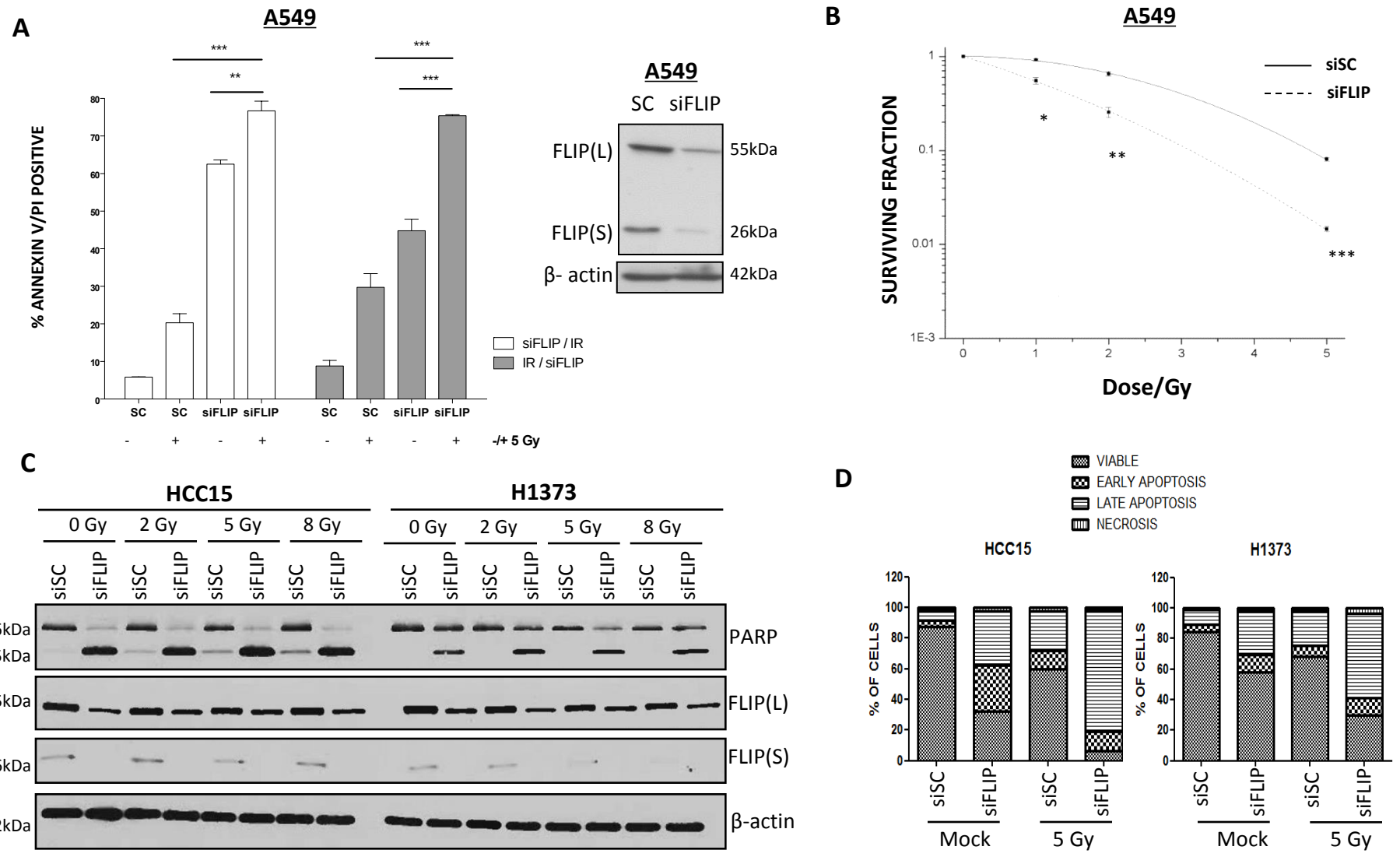
A
A549
% ANNEXIN V/PI POSITIVE
SC SC siFLIP siFLIP SC SC siFLIP siFLIP
-/+ 5 Gy
siFLIP / IR
IR / siFLIP
A549
SC siFLIP
FLIP(L)
FLIP(S)
β- actin
55kDa
26kDa
42kDa
B
A549
SURVIVING FRACTION
Dose/Gy
siSC
siFLIP
C
HCC15
H1373
0 Gy 2 Gy 5 Gy 8 Gy
siSC siFLIP
116kDa
85kDa
55kDa
26kDa
42kDa
PARP
FLIP(L)
FLIP(S)
β-actin
D
VIABLE
EARLY APOPTOSIS
LATE APOPTOSIS
NECROSIS
HCC15
H1373
% OF CELLS
siSC siFLIP siSC siFLIP
Mock 5 Gy

Figure 4

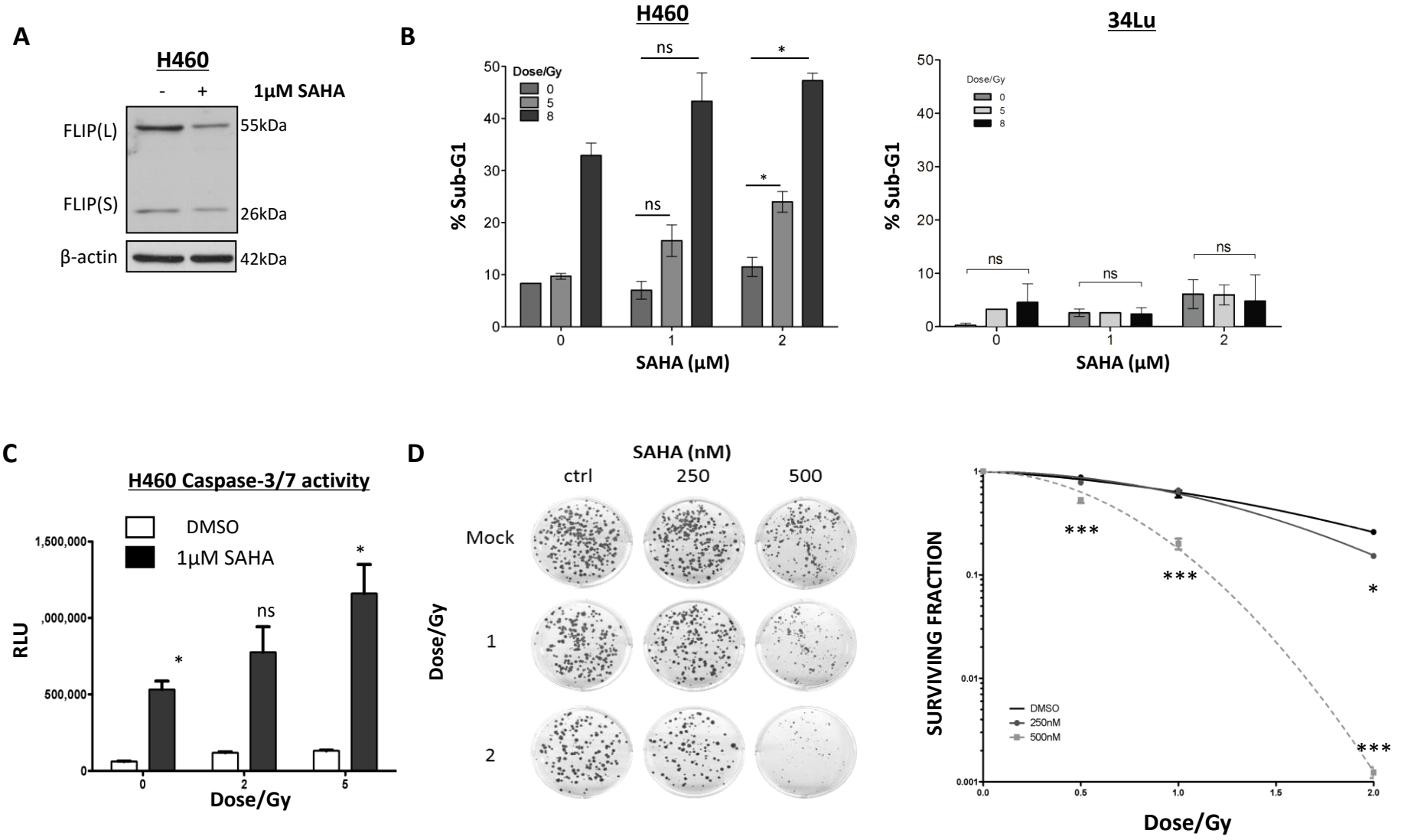
A
H460
- +
1μM SAHA
FLIP(L)
FLIP(S)
β-actin
55kDa
26kDa
42kDa
B
H460
34Lu
Dose/Gy
0
5
8
% Sub-G1
SAHA (μM)
ns
*
C
H460 Caspase-3/7 activity
DMSO
1μM SAHA
RLU
Dose/Gy
D
SAHA (nM)
ctrl
250
500
Mock
1
2
Dose/Gy
SURVIVING FRACTION
DMSO
250nM
500nM
***
*

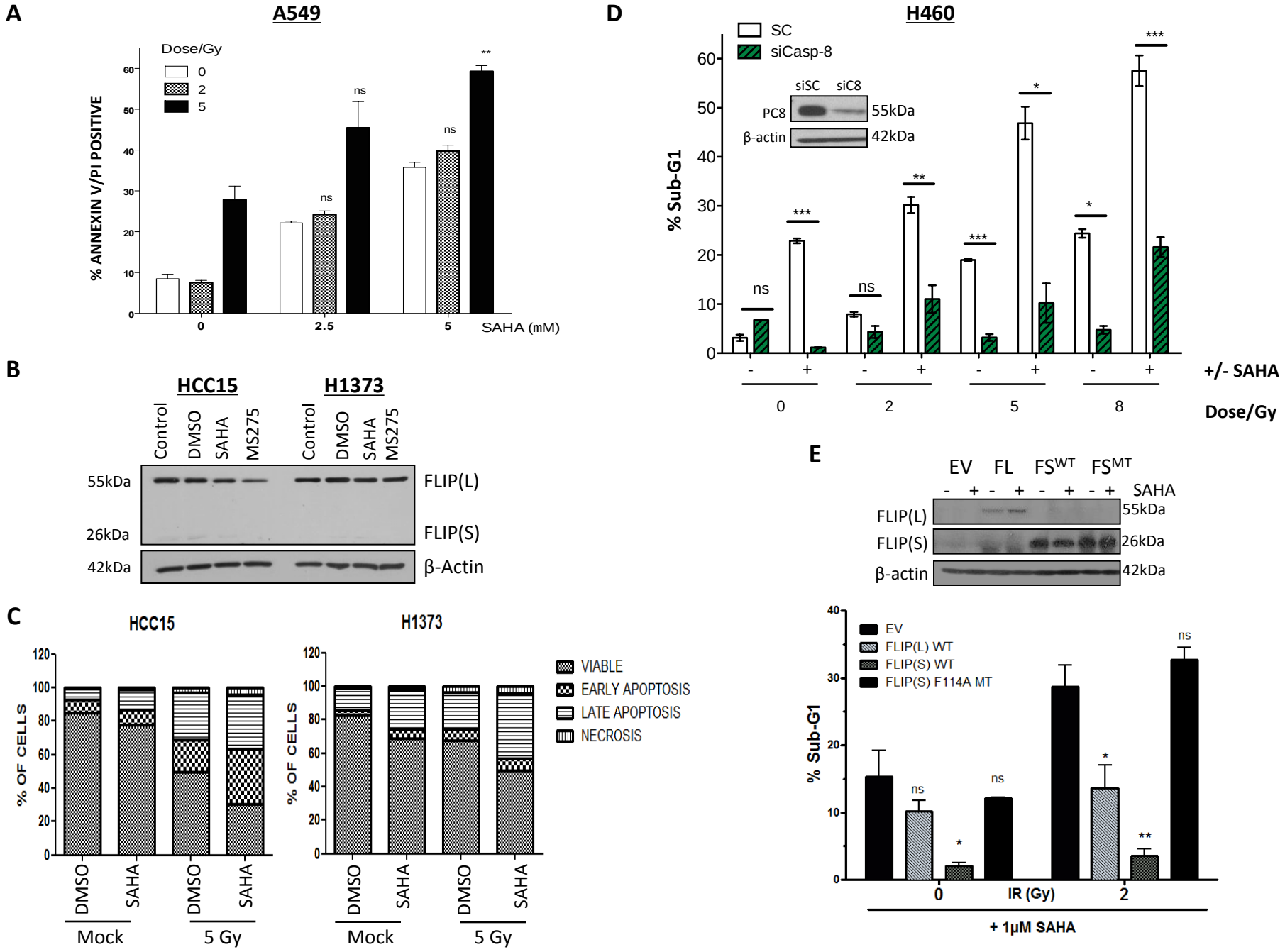
A
A549
Dose/Gy
0
2
5
% ANNEXIN V/PI POSITIVE
ns
ns
ns
**
0
2.5
5
SAHA (mM)
B
HCC15
H1373
Control
DMSO
SAHA
MS275
55kDa
26kDa
42kDa
FLIP(L)
FLIP(S)
β-Actin
C
HCC15
H1373
% OF CELLS
DMSO
SAHA
Mock
5 Gy
VIABLE
EARLY APOPTOSIS
LATE APOPTOSIS
NECROSIS
D
H460
SC
siCasp-8
siSC
siC8
PC8
β-actin
55kDa
42kDa
% Sub-G1
+/- SAHA
Dose/Gy
E
EV
FL
FS^WT
FS^MT
SAHA
FLIP(L)
FLIP(S)
β-actin
55kDa
26kDa
42kDa
EV
FLIP(L) WT
FLIP(S) WT
FLIP(S) F114A MT
% Sub-G1
IR (Gy)
+ 1μM SAHA

Figure 5

Figure 6

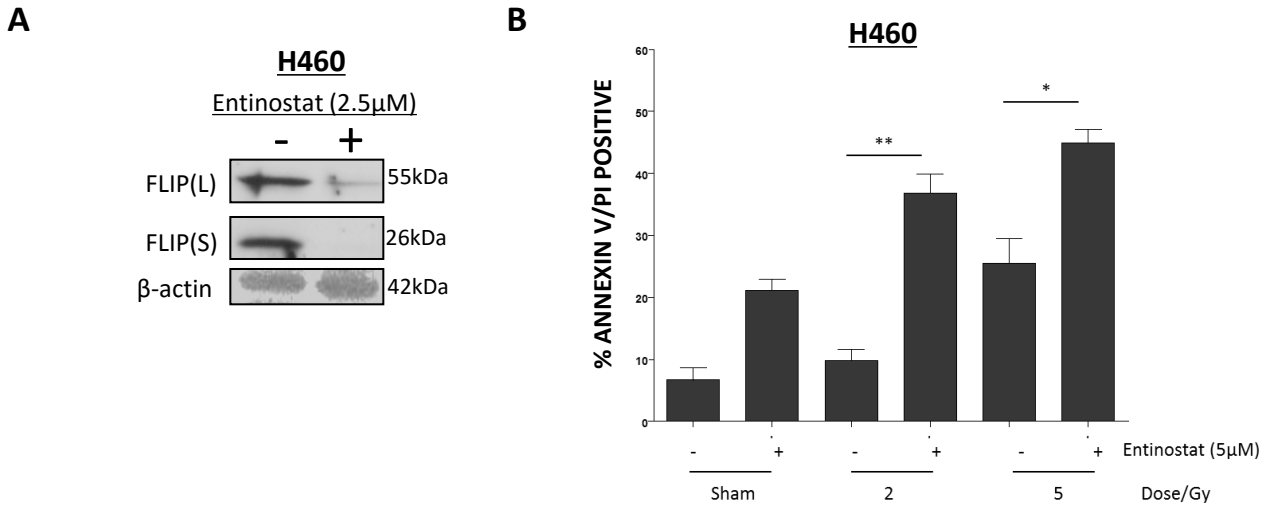
A
H460
Entinostat (2.5µM)
-
+
FLIP(L)
FLIP(S)
β-actin
55kDa
26kDa
42kDa
B
H460
% ANNEXIN V/PI POSITIVE
Entinostat (5µM)
Sham
2
5
Dose/Gy
C
A549
Entinostat (2.5µM)
D
A549
Dose/Gy
Mock
2
5
Entinostat (mM)
E
A549 xenograft model
Tumour Volume (mm3)
Mock
IR
ns (p=0.1)
Vehicle
Entinostat
day 7
day 36